Stathmin/Op18 is a novel mediator of vinblastine activity

Francois Devred[§,*], **Philipp O. Tsvetkov**[‡], **Pascale Barbier**[§], **Diane Allegro**[§], **Susan Band Horwitz**[||], **Alexander A. Makarov**[‡,*], and **Vincent Peyrot**[§]

[§]INSERM 911, CRO2, Aix Marseille University, Faculté de Pharmacie, 27 boulevard Jean Moulin, 13385, Marseille Cedex 5, France

[‡]Engelhardt Institute of Molecular Biology, Russian Academy of Sciences, Vavilov Street 32, 119991 Moscow, Russia

[||]Department of Molecular Pharmacology, Albert Einstein College of Medicine, Bronx, New York 10461, USA

Abstract

Microtubule dynamic instability is tightly regulated by stabilizing and destabilizing proteins, the latter being exemplified by stathmin/Op18, a protein known to destabilize microtubules. Studies in cells have indicated that the level of stathmin expression modifies the cytotoxicity of antimicrotubule drugs, such as vinblastine. Using isothermal titration calorimetry and analytical ultracentrifugation, we show that vinblastine increases the affinity of stathmin for tubulin 50-fold (and *vice versa*). These results are the first biochemical evidence of the direct relationship between stathmin and an antimitotic drug, and reveal a new mechanism of action for vinblastine.

Keywords

1. Introduction

The microtubule cytoskeleton is a dynamic network that plays a crucial role in many cellular processes, including cell division. Microtubules are characterized by their ability to switch abruptly between growing and shortening. This dynamic behaviour, called dynamic instability, guarantees cellular homeostasis and is tightly regulated by stabilizing and destabilizing

[*]To whom correspondence should be addressed. François Devred, Tel: +33491835596. Fax: +33491835505. E-mail: francois.devred@pharmacie.univ-mrs.fr and Alexander Makarov, Tel: +74991354095. Fax:+74991351405. E-mail: aamakarov@eimb.ru

Structured summary
MINT-6603918:
tubulin beta (uniprotkb:Q9H4B7), *tubulin alpha* (uniprotkb:Q71U36) and *stathmin* (uniprotkb:P16949) *physically interact* (MI:0218) by *cosedimentation* (MI:0027)
MINT-6603930:
tubulin alpha (uniprotkb:Q71U36) *physically interacts* (MI:0218) with *tubulin beta* (uniprotkb:Q9H4B7) and *stathmin* (uniprotkb:P16949) by *isothermal titration calorimetry* (MI:0065)

microtubule associated proteins (MAPs). Over the past several decades, significant advancements have been made in our understanding of the mechanism of action of stabilizing MAPs, such as Tau [1-4]. More recently, however, attention has turned to a family of destabilizing molecules: stathmin and its family members that share the same SLD (stathmin like domain), such as RB3 [5].

Stathmin is known to promote microtubule depolymerization by increasing the catastrophe rate (transition from a state of growth to a state of shrinkage) and sequestering free tubulin, thus lowering the pool of "assembly competent" tubulin [6]. A number of reports have shown that stathmin is expressed at high levels in a wide variety of human cancers [7-10]. Furthermore, it has been observed that stathmin modifies the antimitotic efficiency of antitumor cancer drugs, such as vinblastine [11,12]. However, despite a variety of data from cell lines, the molecular basis of this process is not known. Recent crystallographic data suggest that both vinblastine and stathmin might act together, since they can bind simultaneously on free tubulin and each results in the curving of tubulin dimer filaments [13]. In this study, we present the first direct evidence of the functional synergy between endogenous stathmin and the antimitotic drug vinblastine (VLB). Using isothermal titration calorimetry (ITC) and analytical ultracentrifugation (AUC), we demonstrate that vinblastine significantly increases the stathmin binding constant for tubulin and that stathmin has the same effect on the vinblastine binding constant for tubulin. Stathmin can thus be regarded as a novel mediator of cell sensitivity to vinblastine, thereby enhancing its potential as a promising target for cancer therapeutics.

2. Materials and Methods

2.1. Materials

All chemicals (Sigma-Aldrich Co., USA) were of the highest grade. Vinblastine was from Lilly (Suresnes, France). To measure vinblastine concentration we used its molar extinction coefficient at 320 nm in phosphate GTP buffer: $4642\ M^{-1}\ cm^{-1}$ [14].

2.2. Protein purifications

Tubulin was purified from lamb brains by ammonium sulfate fractionation and ion-exchange chromatography and stored in liquid nitrogen as described [1,15]. Tubulin concentration was determined spectrophotometrically at 275 nm with an extinction coefficient of $109\ 000\ M^{-1}\ cm^{-1}$ in 6 M guanidine hydrochloride. Human stathmin was amplified from a pCR 2.1 vector containing the stathmin sequence and introduced in a pET11c (Novagen) vector from which it was expressed in *Escherichia coli* BL21(DE3). Stathmin expression was induced by the addition of 0.4 mM isopropyl 1-thio-D-galactopyranoside (IPTG) to cells when A_{600nm} reached 0.6. After 4 h of induction at 37°C, cells were pelleted and resuspended in 20 mM TrisHCl, 1 mM EDTA, pH 8 containing an antiprotease cocktail (Roche). After two runs in the French press (6 tones), the lysate was cleared by centrifugation (3000 g, 15 min, 4°C), boiled for 5 min, and centrifuged at 100000 g for 1 h at 4°C. This supernatant was loaded onto a HiTrap DEAE-FF column (GE Healthcare) pre-equilibrated with 20 mM Tris HCl, pH 8 and then eluted with the same buffer with additional 200 mM NaCl. Further purification was achieved using a SourceTM 15RPC PE 7.5/150 (GE Healthcare) reverse-phase column equilibrated with H_2O, TFA (0.065%), and eluted with Acetonitrile, TFA (0.05%). Fractions containing stathmin were then pooled and dry-lyophilized. Stathmin was resuspended and its concentration determined by the Lowry method with DC Protein Assay (Bio-Rad) and then adjusted, after ITC experiments, to reach the expected stathmin:tubulin stoichiometry of 0.5 [16].

2.3. Isothermal Titration Calorimetry (ITC)

Binding of vinblastine and stathmin to tubulin was analyzed by ITC using MicroCal MCS or auto-ITC at 10°C in 20 mM NaPi buffer, in the presence of 0.1 mM GTP, pH 6.5. Experimental temperature was chosen to maximize ΔH values and to compare our results with previously published data [16]. Tubulin concentrations in the calorimetric cell ranged from 5 to 20 μM, whereas the ligand (VLB or stathmin) concentrations varied from 50 to 200 μM. Stathmin binding to tubulin was carried out in the presence or absence of VLB and VLB binding to tubulin was carried out in the presence or absence of stathmin. The baseline was measured by injecting the ligand into the protein-free buffer solution. Data were analyzed using the MicroCal Origin software and were fitted with a "one set of sites" and led to the determination of affinity constants (K) and enthalpy changes (ΔH) as previously described [17]. Consequently, the entropy variations (ΔS) were calculated according to the standard equations. The change in heat capacity of binding (ΔCp) was obtained by measuring the change of the binding enthalpy at 5, 10, 15 and 25°C from the relationship $\Delta Cp = \mathrm{d}(\Delta H)/\mathrm{d}T$, assuming that ΔH approximates a linear function of temperature.

2.4. Analytical Ultracentrifugation (AUC)

Experiments were performed at 40,000 rpm and 10°C in a Beckman Optima XL-A analytical ultracentrifuge equipped with absorbance optics, using an eight hole An50Ti rotor and 1.2 cm Epon double-sector centerpieces. Apparent sedimentation coefficients were determined by the sedimentation coefficient distribution C(s) generated by SEDFIT program [18]. All the analytical ultracentrifugation experiments were done in 20 mM NaPi, 10 μM GTP, pH 6.5. Tubulin concentration was 13 μM. All samples for AUC were prepared under the same conditions as for ITC.

3. Results and Discussion

3.1. Oligomeric state of tubulin and its complexes

The oligomeric state of tubulin was monitored by analytical ultracentrifugation. As expected, without vinblastine or stathmin, tubulin sedimented as a single species centered at an apparent sedimentation coefficient S_{app} of 5.08 S (Figure 1, green curve), which corresponds to the usual profile for pure tubulin heterodimers with a standard sedimentation coefficient $S^{\circ}_{20,W}$ of 5.8 S [19]. In the presence of equimolar concentrations of stathmin, these species disappeared in favor of the formation of the typical tubulin-stathmin complex (T2S) sedimenting at a S_{app} of 7.7 S (Figure 1, black curve) [20]. Moreover, in the presence of vinblastine, a wide distribution with a main peak centered at a S_{app} of 9.7S was observed (Figure 1, red curve), corresponding to an equilibrium between tubulin oligomers and several indefinite isodesmic self-associating tubulin polymers induced by the binding of vinblastine [21]. In the presence of stathmin and vinblastine, this wide distribution turned into a single peak at 7.4 S (Figure 1, blue curve), indicating the disassembly of vinblastine-induced tubulin oligomers and the subsequent formation of a T2S-VLB complex. The slight, but reproducible, shift of this peak compared to the T2S one, could suggest that the complex formed in presence of VLB is more compact or that the binding of vinblastine induces a rearrangement of charges at the surface of the complex. The same profile was observed when stathmin was added to tubulin prior to vinblastine, showing that, under our conditions, stathmin is not only able to inhibit VLB-induced polymer formation but also to depolymerize it (Figure 2).

3.2. Thermodynamic parameters of tubulin complex formation

To determine the impact of vinblastine on the thermodynamic parameters of the stathmin - tubulin interaction, ITC was used. A microcalorimetric approach allows the full characterization of this interaction in solution from a thermodynamic point of view [16]. We

first investigated stathmin binding to tubulin in absence (Figure 2, B1) or presence (Figure 2, A2) of vinblastine. Second, we studied vinblastine binding to tubulin in absence (Figure 2, A1) or presence (Figure 2, B2) of stathmin. The thermodynamic parameters found for the tubulin-stathmin interaction (Table 1) are in good agreement with the parameters found by Honnappa *et al.* under similar experimental conditions [16].

We then monitored the binding of stathmin to the tubulin/VLB complex (Figure 2, A2; Figure 3) and found that vinblastine increases stathmin affinity to tubulin more than 15-fold (Table 1). This value is very close to the maximum binding constant that can be reliably measured by ITC for this concentration of tubulin. Thus the stathmin - tubulin binding constant in the presence of vinblastine could be underestimated. Assuming that stathmin would increase the association constant of VLB to tubulin in the same way we tried to get a better approximation of this underestimated constant by measuring the influence of stathmin on VLB binding to tubulin.

By following the binding of vinblastine to tubulin by ITC, we found thermodynamic parameters (Table 1) in the range of previously published data [22,23]. In the presence of stathmin we observed a 50-fold increase in the vinblastine - tubulin binding constant. The fact that vinblastine increases stathmin binding on tubulin, and *vice versa*, is in good agreement with the X-ray structure of the RB3-tubulin complex which revealed that both stathmin and vinblastine binding induce similar conformational consequences, curving consecutive tubulin dimers [13].

According to our AUC and previously published data [6,24], vinblastine and stathmin binding to tubulin are coupled to either tubulin assembly or disassembly (Figures 1 and 2). Since the ITC method registers the integral heat effect from all reactions in the calorimetric cell, it provides us only with apparent thermodynamic parameters. It should be noted that the binding of VLB to T2S complex (Figure 2, B2) is not coupled with tubulin assembly or disassembly and thus all the measured thermodynamic parameters for this process are not apparent. Nevertheless, in spite of assembly / disassembly secondary processes in A1, A2, and B1 equilibria (Figure 2), binding isotherms could be fitted with a simple "one set of sites" model which gave enthalpy values that verify the equation:

$$\Delta H_{A1}^{app} + \Delta H_{A2}^{app} = \Delta H_{B1}^{app} + \Delta H_{B2}$$

This equality, together with AUC data, validate our model presented in Figure 2, which suggests that both paths (A and B) lead to the formation of the same stathmin-tubulin-VLB complex. One of the consequences of this model is a conservation of the product between the stathmin binding constant and the vinblastine binding constant whichever pathway is taken:

$$K_{A1}^{app} \times K_{A2}^{app} = K_{B1}^{app} \times K_{B2}$$

This enabled us to recalculate the previously underestimated K_{A2}^{app} by direct ITC measurement. We found a value of $5.5 \times 10^8 \ M^{-1}$, corresponding to a 50-fold increase in stathmin affinity to tubulin in the presence of vinblastine (instead of the 15-fold estimated above).

It should be noted that at 10°C all observed binding processes described here (Table 1) are entropy driven ($\Delta S > 0$) and enthalpy unfavourable ($\Delta H > 0$), indicating that both vinblastine and stathmin binding to tubulin lead to burying of hydrophobic surfaces [25]. At physiological temperature (37°C) however, ΔH of VLB-tubulin binding was too small to be precisely measured, thus the change in the heat capacity of binding of VLB ($\Delta C_p = d\Delta H/dT$) was

determined as described in the Materials and Methods section (Figure 4). The ΔC_p values for the analyzed complexes are negative: -388 ± 32 cal mol^{-1} K^{-1} for VLB binding to tubulin (Figure 2, A1) and -1052 ± 56 cal mol^{-1} K^{-1} for VLB binding to T2S (Figure 2, B2). Since the VLB site on tubulin is the same in T2S as in VLB-induced oligomers [13], this difference in the ΔC_p observed in the two binding processes (B2 and A1) can be explained by the positive contribution to ΔC_p from the burying of inter-tubulin interface hydrophobic surfaces [26] during VLB-induced tubulin oligomerization. These values of ΔC_p enabled us to calculate $\Delta H = 2$ kcal mol^{-1} for VLB binding to tubulin and $\Delta H = -20$ kcal mol^{-1} for VLB binding to T2S at 37°C. These data indicate that at the physiological temperature stathmin changes the thermodynamic mode of VLB binding to tubulin to an enthalpy-driven one, thus contributing to the observed increase in affinity of VLB to tubulin.

3.3. Biological significance

Overall, our results demonstrate that vinblastine dramatically increases stathmin affinity for tubulin, and *vice versa*. We demonstrated the existence of a second mechanism of action for vinblastine: not only can it directly bind to microtubules and curve protofilaments, but it can also favor stathmin binding, thus enhancing its depolymerizing activity. In addition to being targeted in new anti-cancer strategies, stathmin is also a new mediator of VLB activity. This is the first report to provide a possible biophysical explanation for the increased sensitivity to *Vinca* alkaloids in cells over-expressing stathmin [12]. This mechanism could contribute to *Vinca* alkaloid selectivity for tumor cells in which stathmin is over-expressed compared to normal cells [7-10].

This *in vitro* study using recombinant stathmin enabled us to examine stathmin binding in its non phosphorylated active form. Nevertheless, we know that during the cell cycle and other cellular processes stathmin activity is tightly regulated by phosphorylation, adding an additional level of regulation and complexity to the stathmin-vinblastine-tubulin interactions. We plan to address this regulation in future studies as well as determine if this effect of stathmin is specific for vinblastine or if other antimitotic drugs can interact with endogenous proteins.

Acknowledgments

Abbreviations

ITC	isothermal titration calorimetry
VLB	vinblastine
VFL	vinflunine
T2S	complex of stathmin with two tubulin dimers
MT	microtubule
AUC	Analytical Ultracentrifugation

References

[1]. Devred F, Barbier P, Douillard S, Monasterio O, Andreu JM, Peyrot V. Tau induces ring and microtubule formation from alphabeta-tubulin dimers under nonassembly conditions. Biochemistry 2004;43:10520–31. [PubMed: 15301550]

[2]. Devred F, Douillard S, Briand C, Peyrot V. First tau repeat domain binding to growing and taxol-stabilized microtubules, and serine 262 residue phosphorylation. FEBS Lett 2002;523:247–51. [PubMed: 12123840]

[3]. Sillen A, Barbier P, Landrieu I, Lefebvre S, Wieruszeski JM, Leroy A, Peyrot V, Lippens G. NMR investigation of the interaction between the neuronal protein tau and the microtubules. Biochemistry 2007;46:3055–64. [PubMed: 17311412]

[4]. Buee L, Bussiere T, Buee-Scherrer V, Delacourte A, Hof PR. Tau protein isoforms, phosphorylation and role in neurodegenerative disorders. Brain Res Brain Res Rev 2000;33:95–130. [PubMed: 10967355]

[5]. Charbaut E, Curmi PA, Ozon S, Lachkar S, Redeker V, Sobel A. Stathmin family proteins display specific molecular and tubulin binding properties. J Biol Chem 2001;276:16146–54. [PubMed: 11278715]

[6]. Steinmetz MO. Structure and thermodynamics of the tubulin-stathmin interaction. J Struct Biol 2007;158:137–47. [PubMed: 17029844]

[7]. Curmi PA, Nogues C, Lachkar S, Carelle N, Gonthier MP, Sobel A, Lidereau R, Bieche I. Overexpression of stathmin in breast carcinomas points out to highly proliferative tumours. Br J Cancer 2000;82:142–50. [PubMed: 10638981]

[8]. Friedrich B, Gronberg H, Landstrom M, Gullberg M, Bergh A. Differentiation-stage specific expression of oncoprotein 18 in human and rat prostatic adenocarcinoma. Prostate 1995;27:102–9. [PubMed: 7638082]

[9]. Ghosh R, Gu G, Tillman E, Yuan J, Wang Y, Fazli L, Rennie PS, Kasper S. Increased expression and differential phosphorylation of stathmin may promote prostate cancer progression. Prostate 2007;67:1038–52. [PubMed: 17455228]

[10]. Price DK, Ball JR, Bahrani-Mostafavi Z, Vachris JC, Kaufman JS, Naumann RW, Higgins RV, Hall JB. The phosphoprotein Op18/stathmin is differentially expressed in ovarian cancer. Cancer Invest 2000;18:722–30. [PubMed: 11107442]

[11]. Alli E, Yang JM, Ford JM, Hait WN. Reversal of stathmin-mediated resistance to paclitaxel and vinblastine in human breast carcinoma cells. Mol Pharmacol 2007;71:1233–40. [PubMed: 17272681]

[12]. Iancu C, Mistry SJ, Arkin S, Wallenstein S, Atweh GF. Effects of stathmin inhibition on the mitotic spindle. J Cell Sci 2001;114:909–16. [PubMed: 11181174]

[13]. Gigant B, Wang C, Ravelli RB, Roussi F, Steinmetz MO, Curmi PA, Sobel A, Knossow M. Structural basis for the regulation of tubulin by vinblastine. Nature 2005;435:519–22. [PubMed: 15917812]

[14]. Lee JC, Harrison D, Timasheff SN. Interaction of Vinblastine with Calf Brain Microtubule protein. J Biol Chem 1975;250:9276–82. [PubMed: 1194282]

[15]. Weisenberg RC, Borisy GG, Taylor EW. The colchicine-binding protein of mammalian brain and its relation to microtubules. Biochemistry 1968;7:4466–79. [PubMed: 5700666]

[16]. Honnappa S, Cutting B, Jahnke W, Seelig J, Steinmetz MO. Thermodynamics of the Op18/stathmin-tubulin interaction. J Biol Chem 2003;278:38926–34. [PubMed: 12860982]

[17]. Lafitte D, Lamour V, Tsvetkov PO, Makarov AA, Klich M, Deprez P, Moras D, Briand C, Gilli R. DNA gyrase interaction with coumarin-based inhibitors: the role of the hydroxybenzoate isopentenyl moiety and the 5′-methyl group of the noviose. Biochemistry 2002;41:7217–23. [PubMed: 12044152]

[18]. Schuck P, Rossmanith P. Determination of the sedimentation coefficient distribution by least-squares boundary modeling. Biopolymers 2000;54:328–41. [PubMed: 10935973]

[19]. Na GC, Timasheff SN. Physical properties of purified calf brain tubulin. Methods Enzymol 1982;85 (Pt B):393–408. [PubMed: 7121278]

[20]. Jourdain L, Curmi P, Sobel A, Pantaloni D, Carlier MF. Stathmin: a tubulin-sequestering protein which forms a ternary T2S complex with two tubulin molecules. Biochemistry 1997;36:10817–21. [PubMed: 9312271]

[21]. Na GC, Timasheff SN. Stoichiometry of the vinblastine-induced self-association of calf brain tubulin. Biochemistry 1980;19:1347–54. [PubMed: 7387993]

[22]. Himes RH. Interactions of the catharanthus (Vinca) alkaloids with tubulin and microtubules. Pharmacol Ther 1991;51:257–67. [PubMed: 1784631]

[23]. Lobert S, Ingram JW, Correia JJ. The thermodynamics of vinca alkaloid-induced tubulin spirals formation. Biophys Chem 2007;126:50–8. [PubMed: 16757093]

[24]. Correia JJ, Lobert S. Physiochemical aspects of tubulin-interacting antimitotic drugs. Curr Pharm Des 2001;7:1213–28. [PubMed: 11472263]

[25]. Thomson, JA.; Ladbury, JE. Isothermal titration calorimetry: a tutorial. Wiley West Sussex; 2004.

[26]. Makarov AA, Tsvetkov PO, Villard C, Esquieu D, Pourroy B, Fahy J, Braguer D, Peyrot V, Lafitte D. Vinflunine, a novel microtubule inhibitor, suppresses calmodulin interaction with the microtubule-associated protein STOP. Biochemistry 2007;46:14899–906. [PubMed: 18052208]
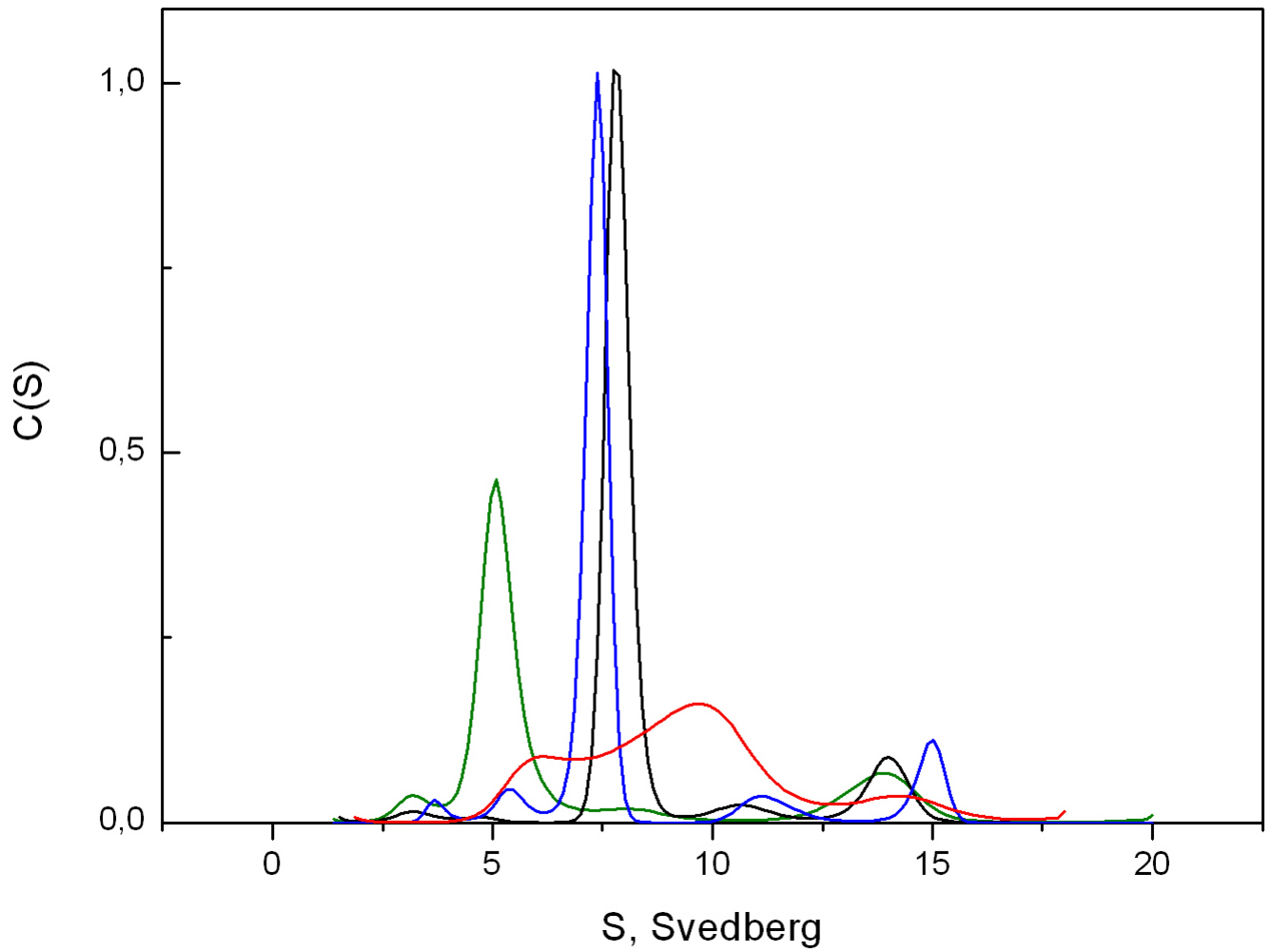
Fig. 1.
Distribution of the sedimentation coefficient c(s) of 13 μM tubulin (green line), 13 μM tubulin with 13 μM stathmin (black line), 13 μM tubulin with 6 μM vinblastine (red line) and 13 μM tubulin with 13 μM stathmin in the presence of 6 μM vinblastine (blue line) at 10°C. All RMSD values were under 0.02.
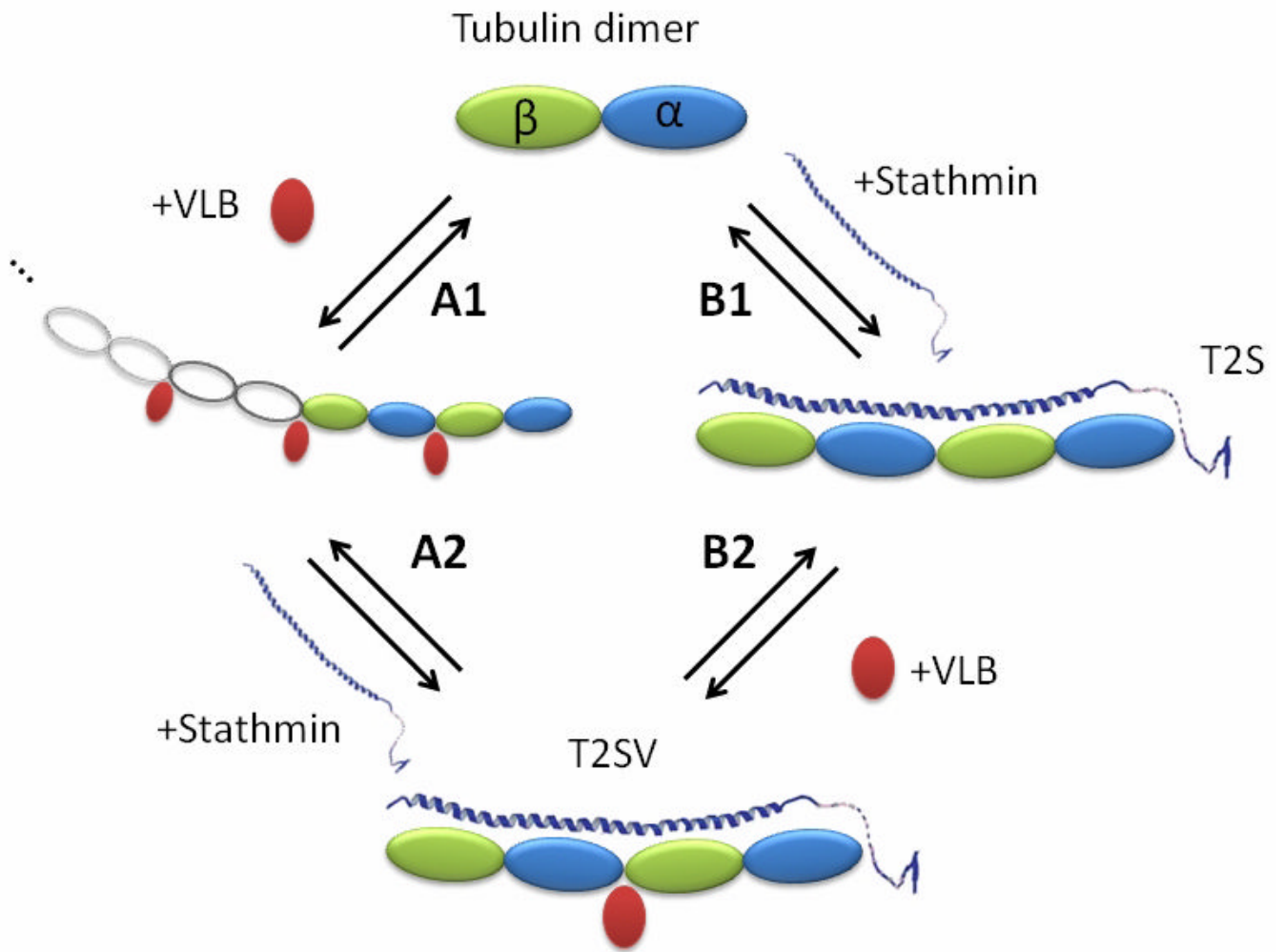
Fig. 2.
Schema of formation of T2S/VLB complex in two different ways: (A) through tubulin/VLB isodesmic indefinite polymer formation; (B) through intermediate T2S complex.
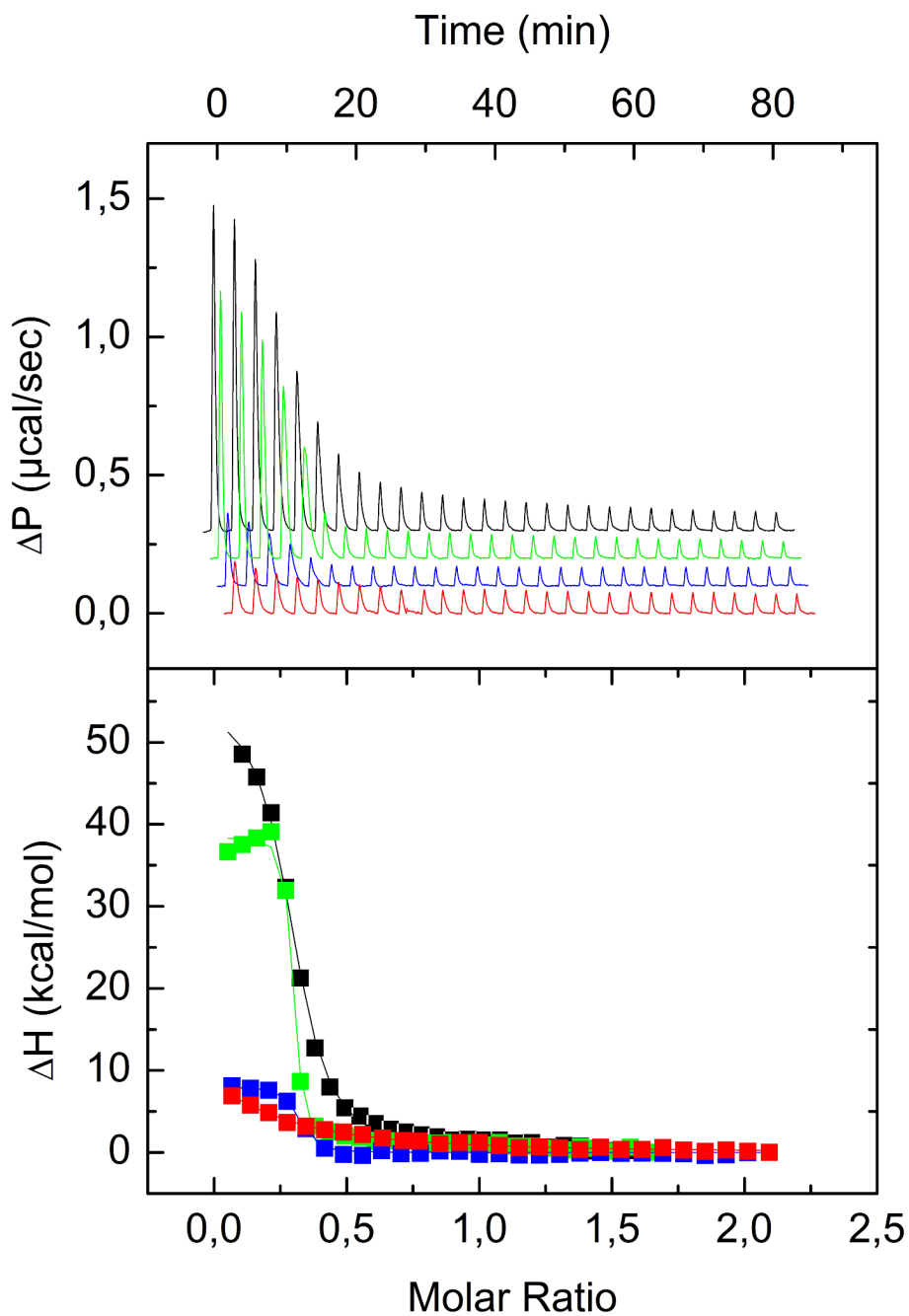
Fig. 3.
ITC curves of VLB and stathmin interaction with tubulin (red and black curves respectively),
VLB interaction with T2S (blue curve) and stathmin binding with tubulin/VLB complex (green
line) at 10°C in 20 mM NaPi buffer in the presence of 0.1 mM GTP, pH 6.5. All four titration
curves were obtained during one set of experiments at Auto-ITC. (A), titration of tubulin or its
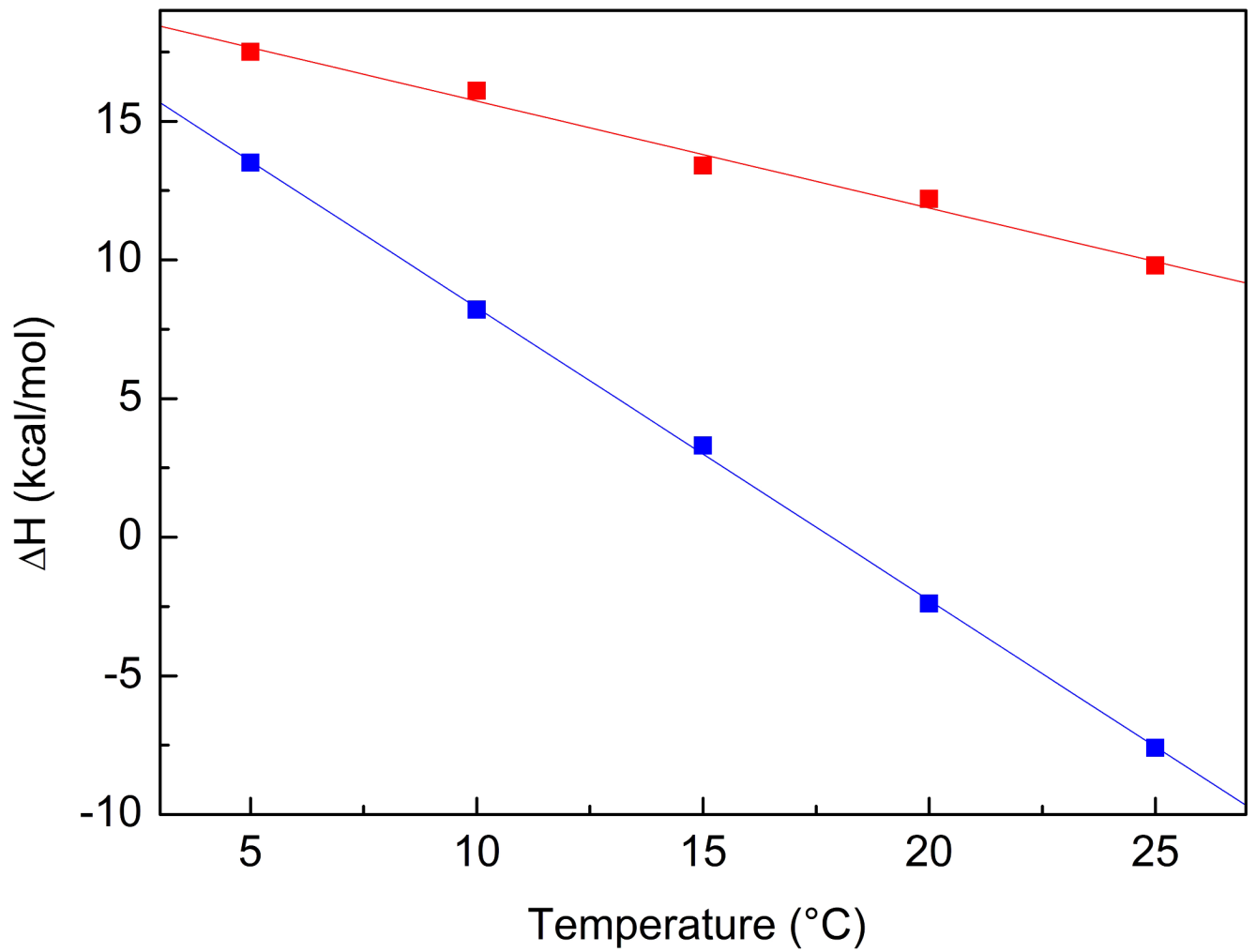complex by the ligand. (B), binding isotherm derived from (A).

Fig. 4.
Temperature dependence of enthalpy of VLB binding to tubulin (A1, red curve) and to T2S
(B2, blue curve) determined by direct ITC measurements.

Table 1

Thermodynamic parameters of VLB and stathmin binding to tubulin and its complex determined by direct ITC measurements at 10°C. A1, B1, A2 and B2 correspond to the reactions presented in Figure 2

	Sample	Ligand	K_{app} M^{-1}	ΔH_{app} kcal/mol	ΔS_{app} cal/K.mol
B1	Tubulin	Stathmin	$(1.1 \pm 0.7) \times 10^7$	31.5 ± 7.9	143 ± 26
A2	Tubulin/VLB	Stathmin	$>(1.6 \pm 1.0) \times 10^8$	23.6 ± 9.6	121 ± 4
A1	Tubulin	VLB	$(5.0 \pm 1.6) \times 10^5$	16.1 ± 2.3	83 ± 8
B2	T2S	VLB	$(2.5 \pm 1.8) \times 10^7$	08.2 ± 0.4	63 ± 2